Supporting Information

Precise morphology control and continuous fabrication of perovskite solar cells using droplet-controllable electrospray coating system

Seung Chan Hong,[a,b,†] *Gunhee Lee,*[a,b,†] *Kyungyeon Ha,*[b,†] *Jungjin Yoon,*[a,b]

Namyoung Ahn,[a,b] *Woohyung Cho,*[b] *Mincheol Park,*[a,b] *and Mansoo Choi*[a,b,*]

[a] Department of Mechanical and Aerospace Engineering, Seoul National University, Seoul 151-742, Republic of Korea

[b] Global Frontier Center for Multiscale Energy Systems, Seoul National University, Seoul 151-744, Republic of Korea

[*] E-mail: mchoi@snu.ac.kr (M. Choi)

[†] These authors contributed equally to this work.

EXPERIMENTAL DETAILS

Visualization of electrospray

In order to obtain electrospray images, we used a system introduced by Park et al.[1,2] The system was configured with a CMOS camera (M3,IDT Inc.) and a Nd:TAG pulsed laser operated at 532 nm (Helios 532-1.5-50; Coherent) with power of 1.5 W and pulse duration of < 1ns for capturing and illuminating. To measure the size of droplets, we used an image processing software (ImageJ, imagej.nih.gov/ij, USA) and a method introduced by Abramoff et al., Schneider et al. and Park. [1,3,4] In order to secure the reliability of the method, we included droplets which were clearly seen as a black dot and over 0.66 of circularity ($4\pi A_P/P^2$, A_P is the area of particle and P is the perimeter of particle).

Fabrication of perovskite solar cells

ITO-coated glass substrates of 2.5 cm × 2.5 cm and 2.5 cm × 10 cm were cleaned with isopropyl alcohol, acetone and deionized water for 15 min, dried with nitrogen gas and stored in a vacuum oven. The substrates were treated with UV-ozone for 30 min to remove any remaining solvent and lower the surface energy.

The PEDOT:PSS (Clevios PVP Al 4083, Heraeus) solution was spin-coated on the UV-ozone treated ITO-glass substrates at 5000 rpm for 40 sec and dried at 150 °C for 20 min. Then, the $MAPbI_3$ perovskite solution was deposited on the substrates through the electrospray system. The perovskite solution was prepared by dissolving PbI_2 (Alfa Aesar)/MAI (synthesized via

reported method)[5] (0.8:1 molar ratio) into DMSO (Sigma Aldrich) at 30 wt%. The substrates were located on the electrically grounded hot-plate which was 60 mm below the nozzle. Temperature of the substrate was 65 °C during the electro-spraying for 2 min and the flow rate of the solution was fixed at 50 μL/hr with the different applied electrical potentials. The deposited substrates were transferred to another hot-plate and post-annealed at 100 °C for 5 min. All electrospray coating and annealing processes were carried out in ambient conditions. After that, the C_{60} (20 nm), BCP (10 nm), LiF (0.5 nm), and Al (150 nm) were sequentially deposited by the thermal evaporator.

Characterization

The *J-V* characteristics were measured by using a source meter (Keithley 2400, Tektronix) under AM 1.5G illumination condition at an intensity of 100 mW/cm^2 with an Oriel S013 ATM solar simulator, calibrated by a KG5 filtered monocrystalline silicon reference solar cell (91150-KG5, Newport). Our devices were measured in room temperature (25 °C) glove box. The forward and reverse scan rates were set to 200 ms per 20 mV. The devices were covered with a metal mask of 1.33 mm^2 to set the active area to 1.77 mm^2. EQE spectra was measured with a Newport IQE200 system equipped with a 300 mW Xenon lamp and a lock-in amplifier. The SEM images of plane-view were obtained by using a field-emission scanning electron microscopy (MERLIN, Carl Zeiss) while the cross-sectional images were obtained with the focused-ion-beam (FIB) system (AURIGA, Carl Zeiss). The XRD analysis was implemented to characterize the crystal structure by using New D8 Advance (Bruker). The EIS measurements of the devices were carried out in one-sun illumination by using an electrochemical potentiostat (CHI 600D, CH Instruments).

Methods	Strength	Weakness
Ultrasonic spray	- Large area fabrication - Continuous fabrication	- Expensive experimental equipment - Complicated setup
Hand spray	- Simple setup - Low cost	- Difficulty in systematic manufacturing
Electric field assisted spray	- Simple setup - Low cost	- Need for post-processing - Difficulty in continuous manufacturing

Table S1. Strengths and weaknesses of existing spray-coating methods

Area	V_{OC} [v]	J_{SC} [mA/cm^2]	FF	PCE [%]
(1)	0.94	16.24	69.98	10.64
(2)	0.97	16.24	73.86	11.65
(3)	0.97	16.45	74.13	11.80
(4)	0.95	16.06	74.81	11.38
(5)	0.96	17.12	72.98	12.00
(6)	0.96	16.74	75.19	12.04

Table S2. Photovoltaic parameters of the six complete devices corresponding to the areas shown in **Figure 4b.**

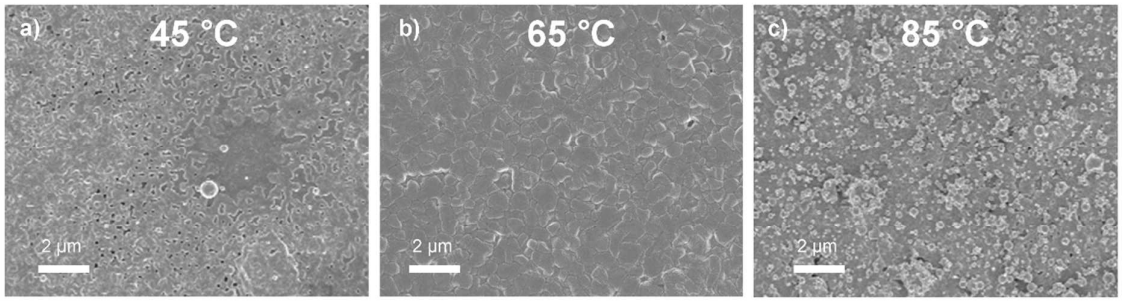

Figure S1. SEM images of the perovskite films fabricated by heating the substrates at (a) 45 °C, (b) 65 °C, and (c) 85 °C

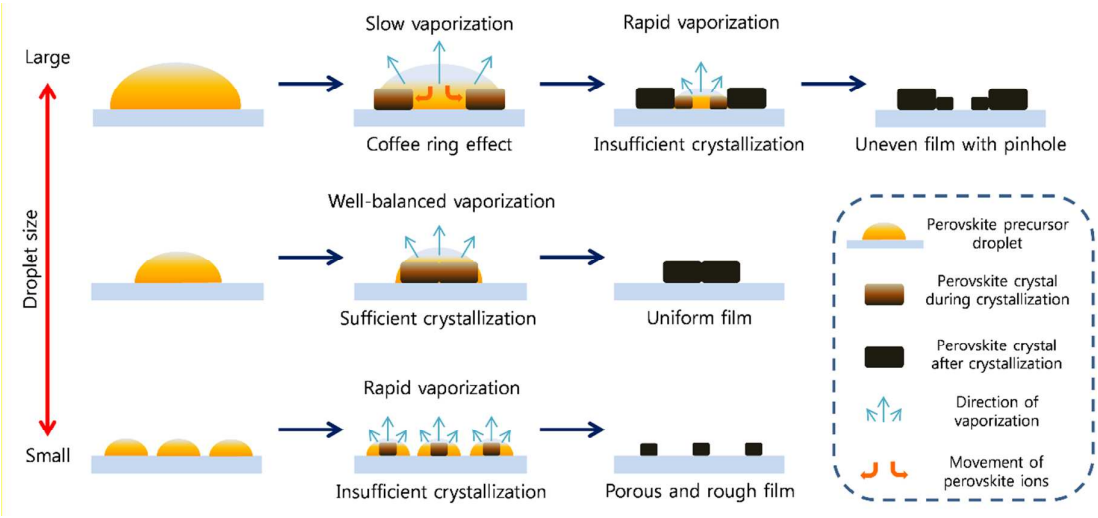

Figure S2. Schematic description of the growth mechanism of perovskite films with respect to the droplet size of the perovskite precursor.

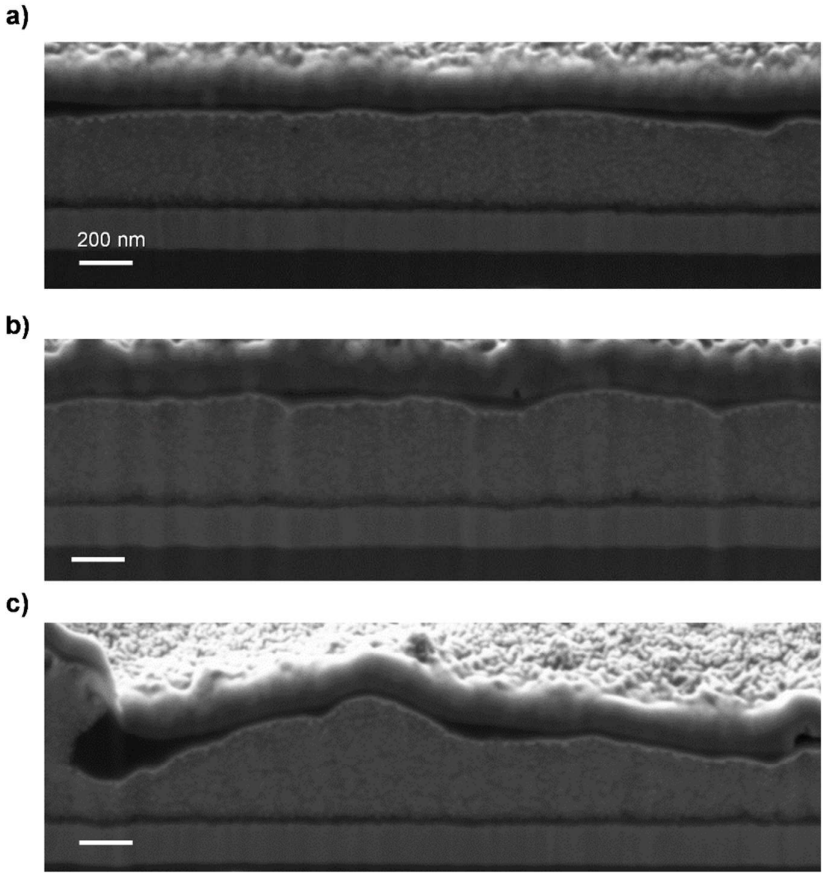

Figure S3. Cross-sectional SEM images of perovskite solar cells under (a) 10.5 kV, (b) 11.5 kV and (c) 12.5 kV conditions.

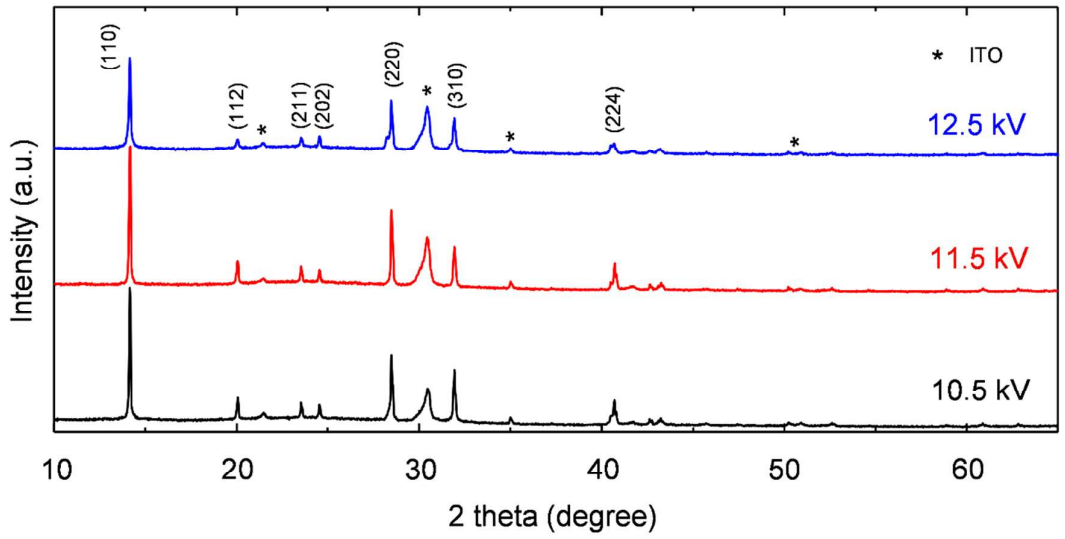

Figure S4. XRD patterns of perovskite films in each cases (10.5 kV, 11.5 kV, and 12.5 kV). The peaks of these XRD patterns correspond to those of spin-coated $MAPbI_3$ films shown in **Figure S5**, which means that the pure $MAPbI_3$ films were formed through our electrospray system. Especially, the (110) and (220) peak intensities in the case of 11.5 kV are much stronger than those of the other cases, indicating that the 11.5 kV film has the highest crystallinity among three cases.[6] Moreover, the 11.5 kV film shows the largest grain size compared to the other films as can be clearly seen in **Figure 2e-g**, which corresponds to the highest crystallinity in the XRD analysis.

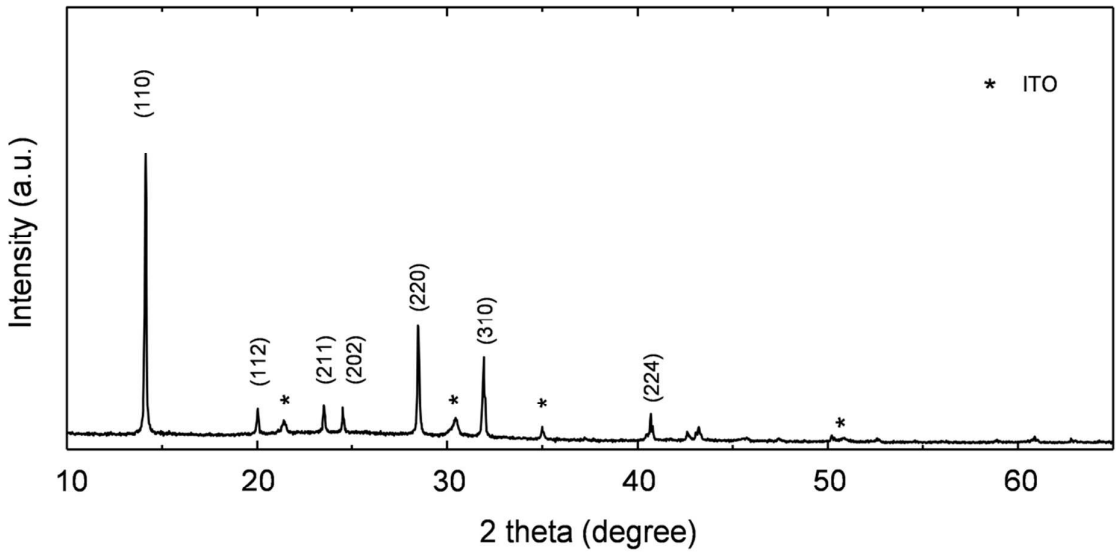

Figure S5. XRD patterns of a perovskite film prepared by spin-coating.

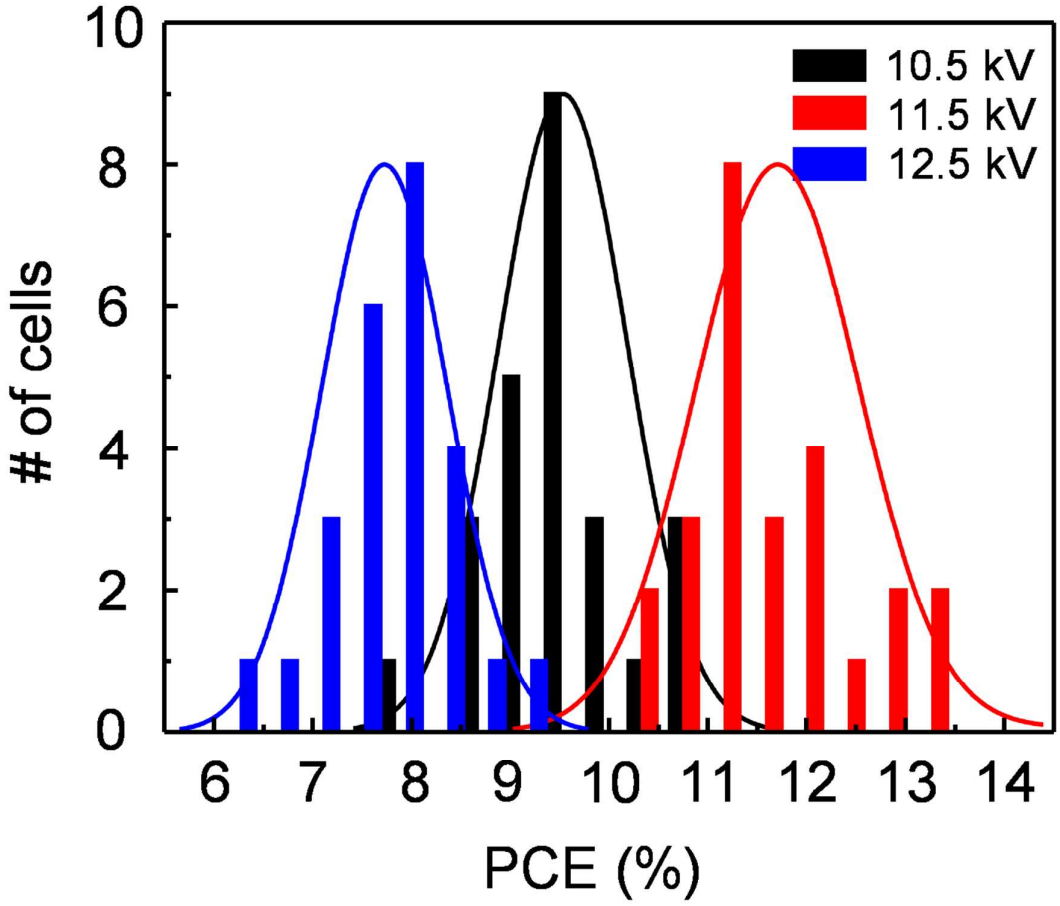

Figure S6. Histograms of PCE of 25 devices depending on the applied electrical potentials.

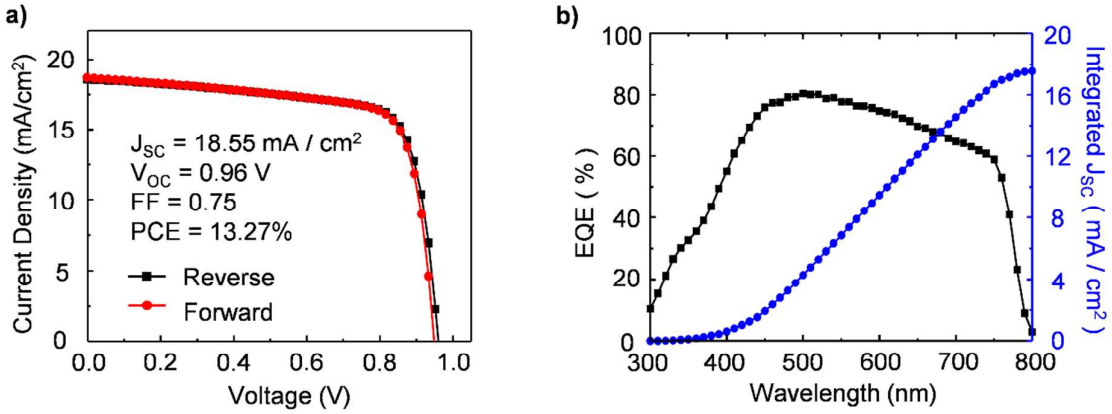

Figure S7. (a) Current-voltage curves of the best performing perovskite solar cell measured in reverse and forward scans. (b) EQE spectra (black) and the integrated J_{sc} (blue)

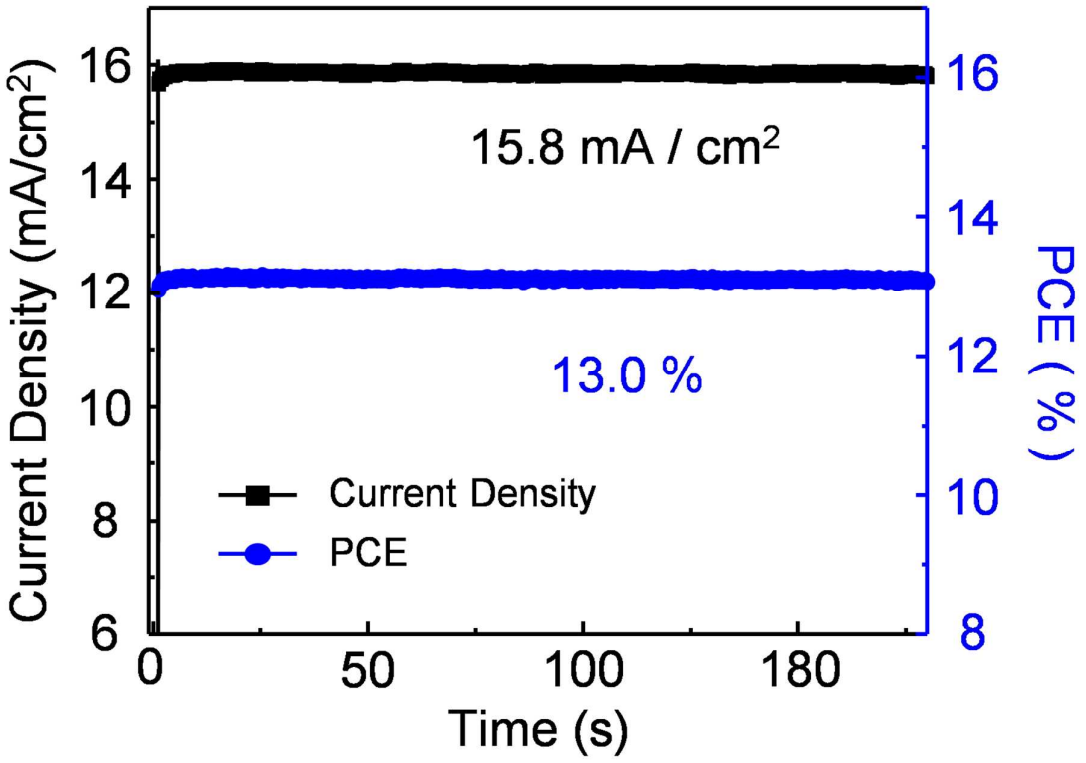

Figure S8. Steady-state photocurrent density (black) and power conversion efficiency (blue) measured at the maximum power voltage of 0.82 V for 200 sec.

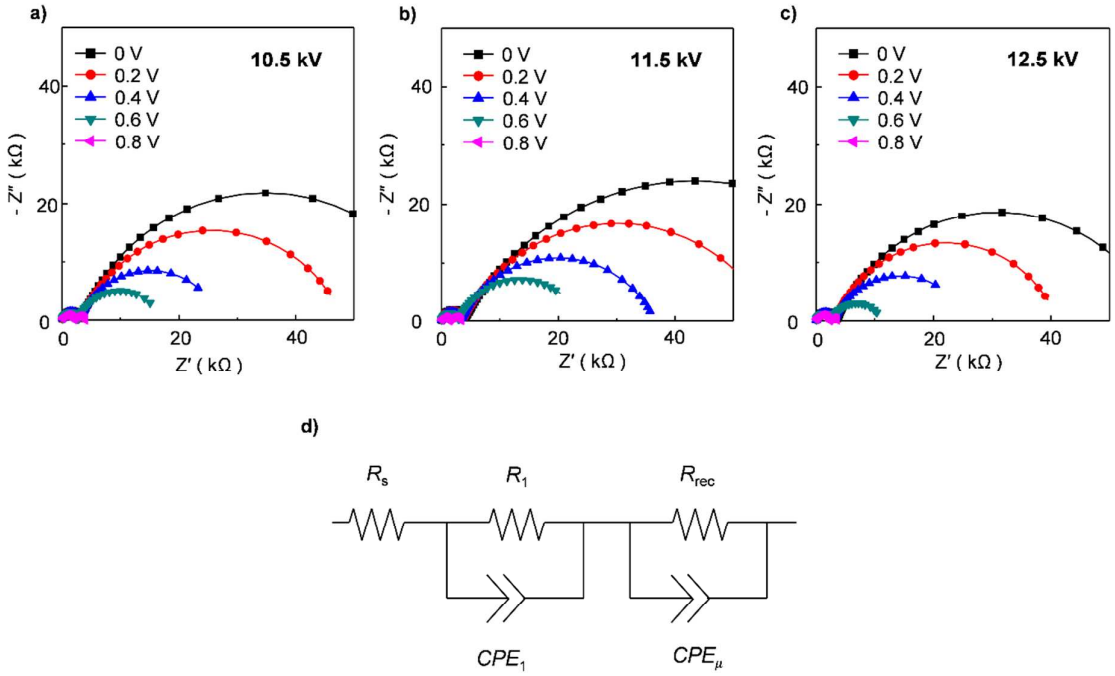

Figure S9. Nyquist plots for the (a) 10.5 kV, (b) 11.5kV and (c) 12.5 kV devices. (d) The equivalent circuit used for data fitting. We obtained EIS spectra of the three types of devices (10.5 kV, 11.5 kV, and 12.5 kV device) in the frequency range from 1 MHz to 0.05 Hz at five bias voltage points (0 V, 0.2 V, 0.4 V, 0.6 V and 0.8 V) under one-sun illumination and fitted the measured data with the simplified circuit model. The semicircles of the high and low frequency regions are commonly associated with charge transfer resistance (R_1) and charge transport-recombination resistance (R_{rec}), respectively.[7-9]

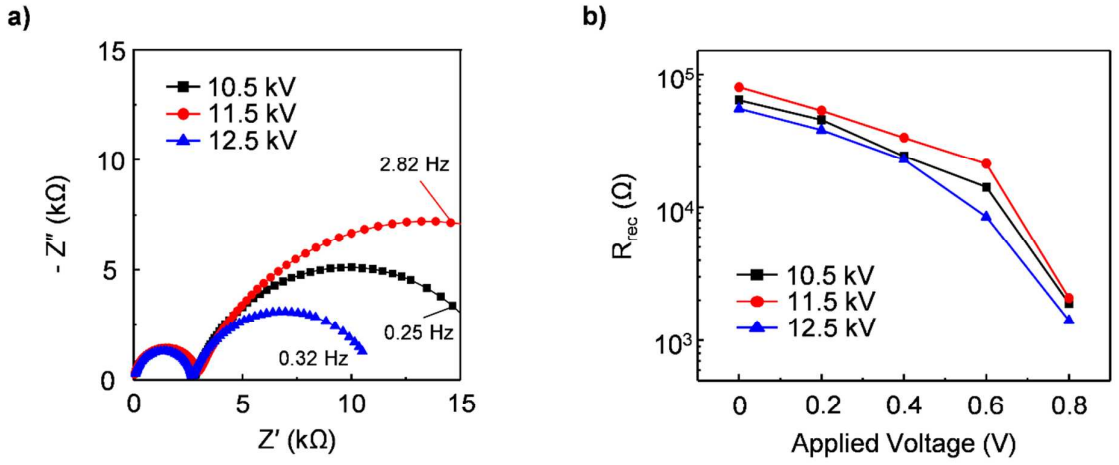

Figure S10. (a) Nyquist plots of three types of device measured under 0.6 V bias voltage. (b) A graph for R_{rec} as a function of the applied voltage. The values of R_{rec} were fitted from EIS data. Since the second semicircles are obviously distinguishable in all cases, we can easily compare R_{rec} from Nyquist plots. The second semicircle of the 11.5 kV device is larger than those of other devices, which is attributable to decreased recombination loss (**Figure S10a**). Regardless of the applied bias voltage, the R_{rec} value of the 11.5 kV device is higher than those of the other devices (**Figure S10b**). Generally, the pinholes of the perovskite film cause the carrier recombination due to direct contact between the hole and electron transport layers, and the grain boundaries provide carrier trap centers.[9] As mentioned in manuscript (**Figure 2**), the 11.5 kV devices have pinhole-free and large grain-sized perovskite films, which results in the decreased recombination loss. Consequently, the EIS characterization explains why the 11.5 kV devices have improved photovoltaic parameters as powerful evidence with respect to recombination loss.

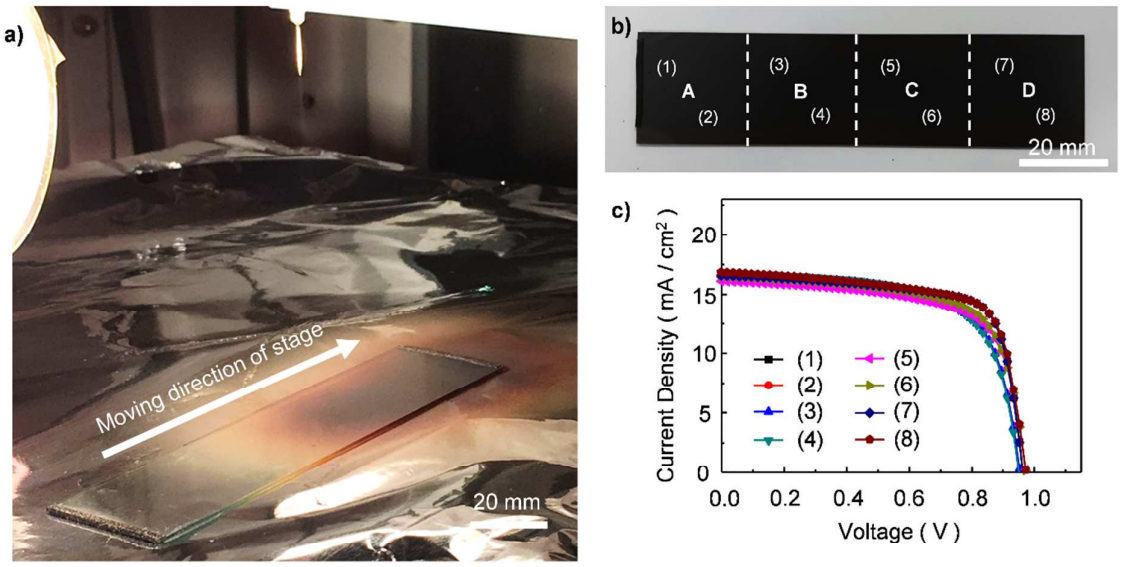

	V_{OC} [V]	J_{SC} [mA/cm²]	FF	PCE [%]
Average	0.97 ± 0.01	16.58 ± 0.21	69.09 ± 3.00	11.06 ± 0.55

Figure S11. (a) Photograph of the continuous electrospray coating system with perovskite films being produced. (Substrate size: 2.5 x 10 cm, Moving speed of the stage: 1.25 cm/min) (b) Photograph of fabricated perovskite films with eight different areas marked. (c) Current-voltage curves of perovskite solar cells in each marked area.

REFERENCES

(1) Park I., Experimental Study on Water Electrospray: Characteristics of Jet Instability and Droplet Generation. PhD thesis, Korea Advanced Institute of Science and Technology, June, **2015**

(2) Park, I.; Kim, S. B.; Hong, W. S.; Kim, S. S., Classification of Electrohydrodynamic Spraying Modes of Water in Air at Atmospheric Pressure. *J. Aerosol Sci.* **2015,** *89*, 26-30.

(3) Schneider, C. A.; Rasband, W. S.; Eliceiri, K. W., NIH Image to ImageJ: 25 Years of Image Analysis. *Nat. Methods* **2012,** *9*, 671-675.

(4) Abràmoff, M. D.; Magalhães, P. J.; Ram, S. J., Image Processing with ImageJ. *Biophotonics international* **2004,** *11*, 36-42.

(5) Kim, H. S.; Lee, C. R.; Im, J. H.; Lee, K. B.; Moehl, T.; Marchioro, A.; Moon, S. J.; Humphry-Baker, R.; Yum, J. H.; Moser, J. E.; Gratzel, M.; Park, N. G., Lead Iodide Perovskite Sensitized All-Solid-State Submicron Thin Film Mesoscopic Solar Cell with Efficiency Exceeding 9%. Sci. Rep. 2012, 2, 591.

(6) Sung, H.; Ahn, N.; Jang, M. S.; Lee, J.-K.; Yoon, H.; Park, N.-G.; Choi, M., Transparent Conductive Oxide-Free Graphene-Based Perovskite Solar Cells with over 17% Efficiency. *Adv.Energy Mater.* **2016,** *6*, 1501873.

(7) Liu, J.; Gao, C.; He, X.; Ye, Q.; Ouyang, L.; Zhuang, D.; Liao, C.; Mei, J.; Lau, W., Improved Crystallization of Perovskite Films by Optimized Solvent Annealing for High Efficiency Solar Cell. *ACS Appl. Mater. Interfaces* **2015,** *7*, 24008-24015.

(8) Christians, J. A.; Fung, R. C.; Kamat, P. V., An Inorganic Hole Conductor for Organo-Lead Halide Perovskite Solar Cells. Improved Hole Conductivity with Copper Iodide. *J. Am. Chem. Soc.* **2014,** *136*, 758-64.

(9) Tai, Q.; You, P.; Sang, H.; Liu, Z.; Hu, C.; Chan, H. L.; Yan, F., Efficient and Stable

Perovskite Solar Cells Prepared in Ambient Air Irrespective of the Humidity. *Nat. commun.* **2016,** *7*, 11105.